Mapping the ASFs of the Northwest European Loran-C System

Paul Williams and David Last

(*University of Wales, Bangor*)

Loran-C receivers measure time delay differences in the signals they receive, compute differences of distance, and hence determine the user's position. The conversion from time to distance requires knowledge of the signals' velocities, which differ when propagating over sea or land. Precise positioning requires the delays of land paths to be accurately mapped, a procedure traditionally entailing expensive and time-consuming marine surveys. The resulting data, in the form of Additional Secondary Factors (ASFs), may be stored in Loran receivers. This paper introduces the concept of Loran-C Additional Secondary Factors, and shows how it is possible to map them efficiently. It focuses on recent advances, chiefly the development of powerful software for modelling the growth of ASFs over mountainous terrain. This employs an implementation of an algorithm proposed by Monteath. The modelling capability of the algorithm is demonstrated by examining propagation along a route that crosses mountains and deep fjords. In addition, the ASFs it predicts are compared with sample measurements made around the west coast of Scotland.

KEY WORDS

1. Loran-C. 2. Corrections. 3. Modelling.

1. INTRODUCTION. The Northwest European Loran-C System (NELS) consists of 9 transmitter stations arranged in 4 chains (Figure 1). Four stations, Bø and Jan Mayen in Norway, Ejde on the Faeroe Islands and Sylt in Germany, are former United States Coast Guard (USCG) installations, transferred to the host nations in 1994. Lessay and Soustons are French military stations. Vaerlandet and Berlevåg in Norway, and the proposed station at Loop Head in Ireland, are new installations. NELS is controlled by a Steering Committee with representatives from the 6 member nations, Denmark, France, Germany, Ireland, The Netherlands and Norway. Non-member, but interested, parties such as the United Kingdom contribute as observers. To implement decisions taken by the Steering Committee, a Co-ordinating Agency Office has been established by the Norwegian Defence Communications and Data Services Administration (NODECA) acting on behalf of the Royal Norwegian Ministry of Fisheries. Each member nation has also set up a National Operating Agency (NOA) to implement Loran-C policy and operations.

2. ASFs IN LORAN-C. Conventionally, Loran-C receivers calculate their positions by measuring the differences in the times of arrival of pulsed signals from pairs of transmitters, so establishing hyperbolic lines of position. The speed of the ground-wave signals that form the components of each time difference varies according to the type of surface over which they travel; the key parameter is the electrical conductivity of the surface. Signals travel most slowly over ice, deserts or

https://doi.org/10.1017/S0373463300008778 Published online by Cambridge University Press

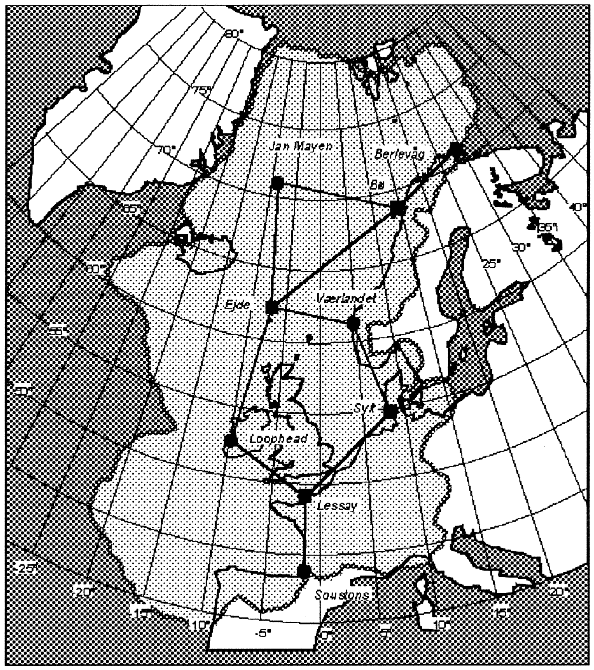

Figure 1. Coverage area of NELS.

mountains, a little more quickly over good farming land and most quickly of all over sea-water. Further, the velocity of propagation of the signals varies with distance from the transmitter in a complicated manner.

Loran-C receivers assume, in the first instance, that the signals they receive have travelled over sea-water paths. They use the USCG *Salt-Water Model*[1] to compute their positions. This model breaks the velocity of a signal travelling over sea-water down into two components: the *primary factor*, or velocity in the earth's atmosphere; and the *sea-water secondary factor*. This secondary factor, the extra delay due to the signal travelling over the sea, is assumed to vary with range, over sea-water of 5000 mS/m conductivity.[2] At this level, receivers know nothing of land-masses. It is necessary, therefore, to determine the additional delays due to the presence of land along the transmission paths if the published absolute accuracy of Loran-C (0·25 nm or 463 m) is to be met. These land delays are the *Additional Secondary Factors*, or ASFs.

The traditional method of determining ASFs is to compare, on a survey vessel or land vehicle, the true position using surveying methods and the position given by a Loran receiver; the differences give the ASFs. However, this method is slow and expensive. It has been estimated that to cover an area the size of NELS would take some 1000 days and cost US$5M. A more cost-effective method would be to compute ASFs from knowledge of the conductivity of the surface. The basic principle of the proposal for mapping the ASFs of the NELS area, outlined in this paper, is to model the ASFs as far as possible, then adjust the resulting values using as sparse a set of measurement points as will give valid corrections. Furthermore, to the maximum extent possible, these measurements will be collected by automatic measuring systems installed on *ships of opportunity*; that is, vessels sailing their normal routes.

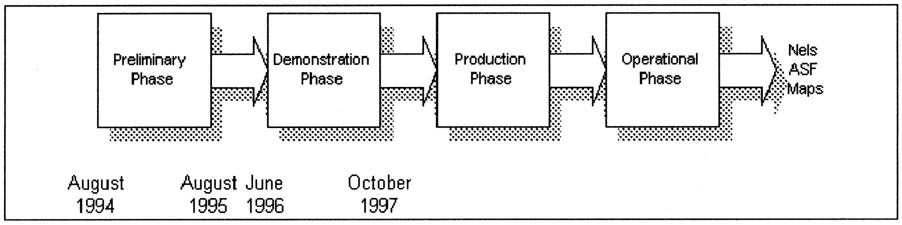

Figure 2. The four phases of the project.

3. PROJECT ORGANISATION AND HISTORY.

The project is being conducted in the four phases shown in Figure 2. The Preliminary Phase explored the principles of the proposed approach and specified the requirements for the succeeding phases.[3]

The work of the Demonstration Phase, a proof-of-concept operation, was split into hardware and software components. The hardware component was undertaken initially by Geometrix A/S (Norway), who developed a specialised measurement system and undertook field trials.[4] Much of their responsibility recently passed to Mors (France), who are currently developing an improved measuring system. This is required to perform the challenging task of determining the ASF values of the signals from individual stations, the so-called *Time of Arrival* (*TOA*) *ASFs*. These are much more difficult to measure accurately than the normal *Time Difference* (*TD*) *ASFs*, which are readily available from conventional Loran receivers.[5] To date, high-quality TOA ASF measurements have not been produced; the software component of the work, on which this paper focuses, is continuing apace in anticipation of their shortly becoming available.

4. ASF MODELLING.

Major objectives of the software component of the project, for which the University of Wales, Bangor, is responsible, are the creation of computer models that generate maps of ASF values for each individual station, and the development of techniques for adjusting these modelled ASFs using sparse measured TOA ASF data. In the Preliminary Phase of the project, it was realised that geographical regions could be classified into two distinct types: technically *easy* and technically *difficult*. In *easy* areas the land is relatively flat, with very little variation of the topography. ASF values in these smooth earth areas can be predicted from knowledge of the ground conductivity alone, using published curves that relate secondary factor to conductivity.[2] The Millington–Pressey algorithm is employed to take account of paths with non-uniform conductivity.[6,7] We have demonstrated software for generating ASF maps of *easy* areas that draws on a digital database of ground conductivity values.[8] Improved resolution of the conductivity database is provided at coastlines, where the conductivity contrast is the greatest, by a coastline database.[9]

We have also successfully used a dataset of ASF values (of somewhat limited extent and quality) recorded by Geometrix during a field trial in an *easy* sea-trial area, to adjust our modelled values. The result showed good agreement between model and measurement and confirmed the underlying principle of the project.[4,5,10] *Difficult* areas are mountainous regions, such as Scotland or Norway, in which the ASF is influenced by variations in topography and so a model based on ground conductivity

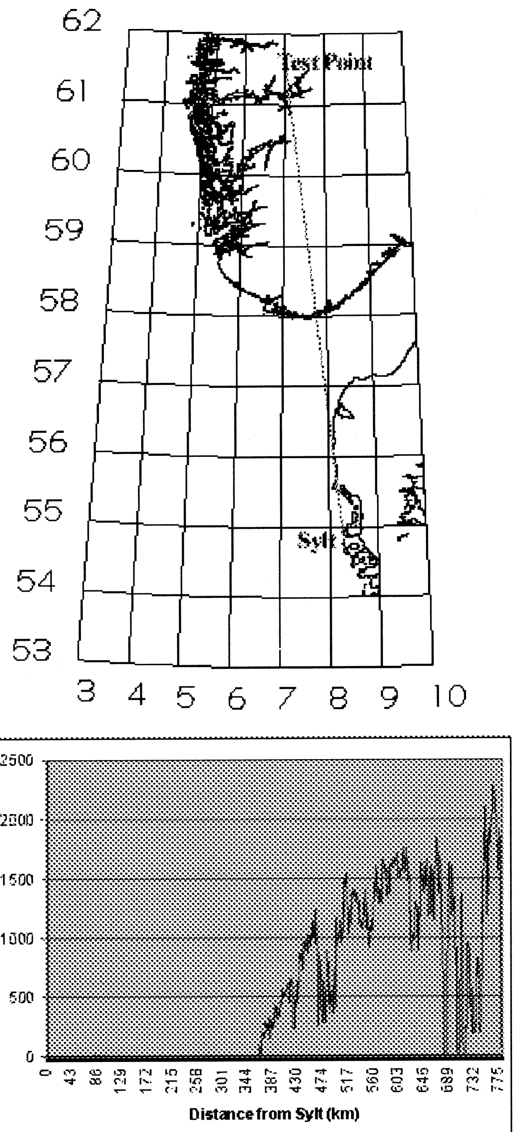

Figure 3. (a) Path from Loran station at Sylt (Germany) to a point in the *difficult* sea-trial area. (b) Terrain elevation profile along the path.

alone is inadequate. Here we require the assistance of a Digital Terrain Database, and a much more advanced computer model. The development of these techniques, which has dominated our work over the last year, will now be described.

5. ASF MODELLING IN *DIFFICULT* AREAS. The subject of groundwave propagation over imperfectly-conducting paths has been studied since the beginning of the century. Much of the early work concentrated on a smooth, plane, homogeneous (ie single conductivity) Earth. Extending these theories to a spherical earth was not a simple process; however, Norton succeeded in reducing the *classical*

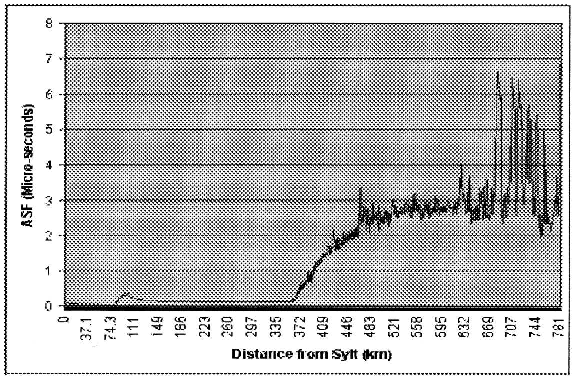

Figure 4. Variations of the ASF of the Sylt signal along the path in Figure 3.

plane-Earth theories to a convenient form. The complicating effects of inhomogeneous, or mixed conductivity, ground and of terrain elevation variations have been studied by numerous workers.[11,12] The method most readily understood by engineers is that resulting from the application of the *Compensation Theorem* (see Reference 13, p. 16); and it is this method which Monteath chose in formulating his solution to this difficult problem.[14] The resulting integral equation is essentially the same as the better-known one published earlier by Hufford.[15] Both employ the simplifying assumption that variations in terrain across the propagation path are negligible. In this way, they reduce a two-dimensional surface integral to a one-dimensional line integral along the propagation path from transmitter to receiver. They then sum at the receiver the contributions of the components of the groundwave reflected from the surface of the earth at a series of points along the propagation path. The result is the complex attenuation factor of the surface of the Earth over which the groundwave has travelled from transmitter to receiver. The method encompasses the effects of both conductivity and topography.

Monteath devised a numerical algorithm for computing his integral. We have taken this algorithm and implemented it in the 'C' programming language. We have tested the resulting code by attempting to reproduce independently Monteath's own test results; the agreement was excellent. In addition, we have tested the algorithm against results obtained by Johler and Berry, who employed a similar integral-equation algorithm to investigate the effects of irregular terrain on the performance of Loran-D.[16] Johler and Berry took as their test model a Gaussian-shaped hill, of a specific conductivity a certain distance from the transmitter; our results agreed with theirs to within 1 dB in magnitude.[5] Samaddar[17] presents a comparison of the integral-equation technique with measured data collected by the US Coast Guard between December 1977 and February 1978 in the West Coast Loran-C coverage area of the United States. The results of Samaddar's comparison shows that the integral-equation technique more closely matched the measured data than the smooth Earth theory of Millington-Pressey, and is considered to be the best available technique.

We then wrote software that allowed the integral algorithm to take data from our digital database of ground conductivity, our coastline database and a highly-detailed topographical database. This we constructed from the US National Imagery and Mapping Agency's Digital Terrain Elevation Data Level 1 (DTED1).[18] It has a resolution of 90 m, approximately equivalent to that of the contour information on

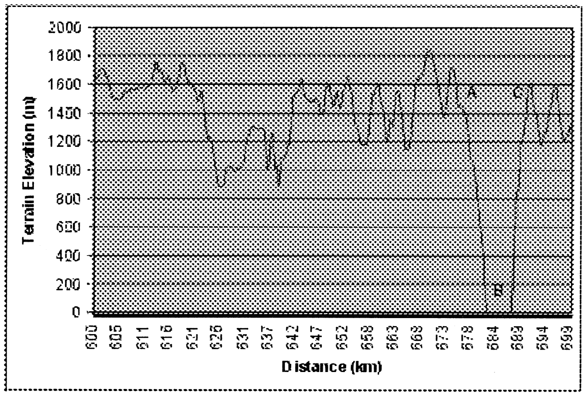

Figure 5. Terrain profile of the 100 km segment of the path crossing the Sognefjorden, between A and C.

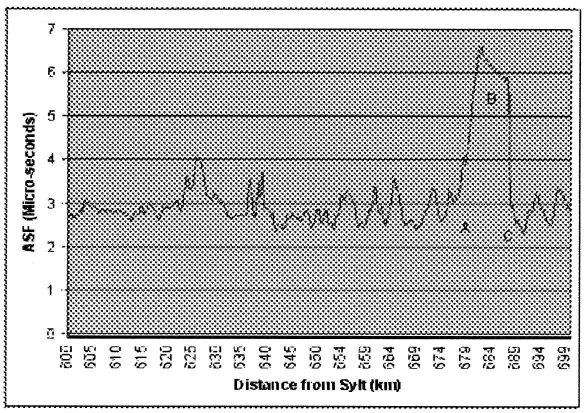

Figure 6. ASF profile along the 100 km segment in Figure 5 of the test path from Sylt.

a 1:250000-scale map. Our software works by reading a list of latitude and longitude co-ordinate pairs from a file. Typically these co-ordinates represent a grid of points at regular intervals across the surface of the Earth. At each point the software accesses the conductivity, coastline and terrain elevation databases. It constructs ground conductivity and terrain height profiles along the propagation path from the transmitter to the point. These two profiles, which may represent substantial variations of conductivity and height, are then divided into a number of integration intervals. At each interval point, the complex groundwave attenuation factor is calculated and stored in a list, which thus contains a profile of this variable along the path. We, of course, are interested in the phase, rather than the magnitude, of the list's elements. We use them to calculate the signal delay at the Loran-C centre frequency of 100 kHz. From the result, we subtract the sea-water delay of a path of the same length. The resulting difference is the ASF value, for that transmitter, at that point.

5.1. *An example path.* As an example of this software model working, we will use it to predict ASF values along the exceptionally difficult path shown in Figure 3. The path starts at the Loran-C station at Sylt (Germany) and runs for 780 km to a

https://doi.org/10.1017/S0373463300008778 Published online by Cambridge University Press

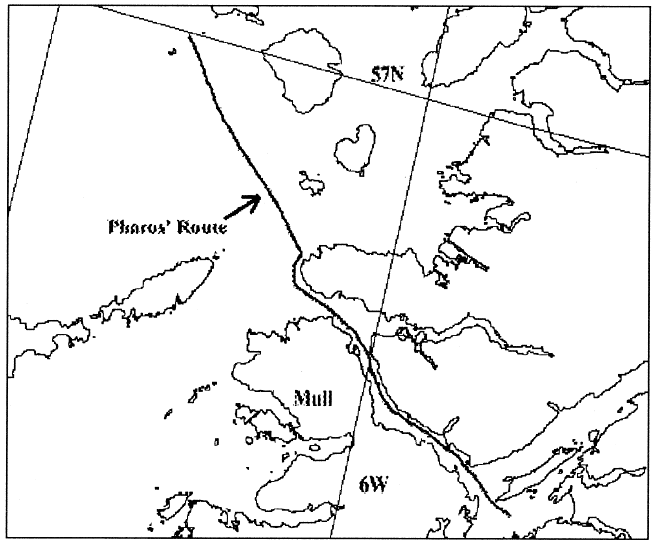

Figure 7. DGPS track of *MV Pharos*' passage through the Sound of Mull off the west coast of Scotland.

point in Norway within the area in which it is hoped soon to conduct *difficult area* sea trials. The path has been chosen because it crosses mountains and narrow fjords, with rapid changes of elevation of some 2000 m over short distances.

The ASF profile of the path, computed using our software, is illustrated in Figure 4. Following a short land section, where approximately 300 ns of ASF is accumulated and then partially lost by coastal recovery,[7,8] the signal travels over the sea until it reaches the Norwegian coastline, approximately 360 km from Sylt. Thereafter, the ASF increases relatively rapidly over the low-conductivity land, attaining a value of about 3 μs before reaching the area of the coastal fjords where it starts to vary dramatically. We will now focus in on that region, examining in detail the effect of a particular fjord, the Sognefjorden.

Figure 5 shows the variations of terrain elevation along the section of the path between 600 and 700 km from Sylt. When we reach the edge of the Sognefjorden (point *A*), the elevation drops from almost 1700 m to sea-level (point *B*) in a distance of 7 km. The ASF (Figure 6) suddenly increases from 3·15 to 6·55 μs over this short distance. Physically, this may be thought of as being due to the signal having to travel the extra distance from the lip of the fjord down to the sea surface. The fjord is about 5 km wide, sufficient for the ASF to fall somewhat as we travel across to the other side. This may be due to a reduction in the extra path length or to the coastal recovery effect. As we climb out of the fjord (to point C) the ASF falls rapidly to a value of 2·95 μs, similar to that just before the fjord.

This example illustrates the dramatic variations of ASF likely to be found in Norwegian fjords and other regions of rapidly changing terrain elevation. They are due to the additional path lengths imposed by topography that cause signal delays in addition to the cumulative growth of ASF over land of low conductivity.

An important practical issue to be considered when computing ASFs using integral-equation methods is the size of the integration interval to be used; its choice is a compromise between faster computation (larger intervals) and higher accuracy

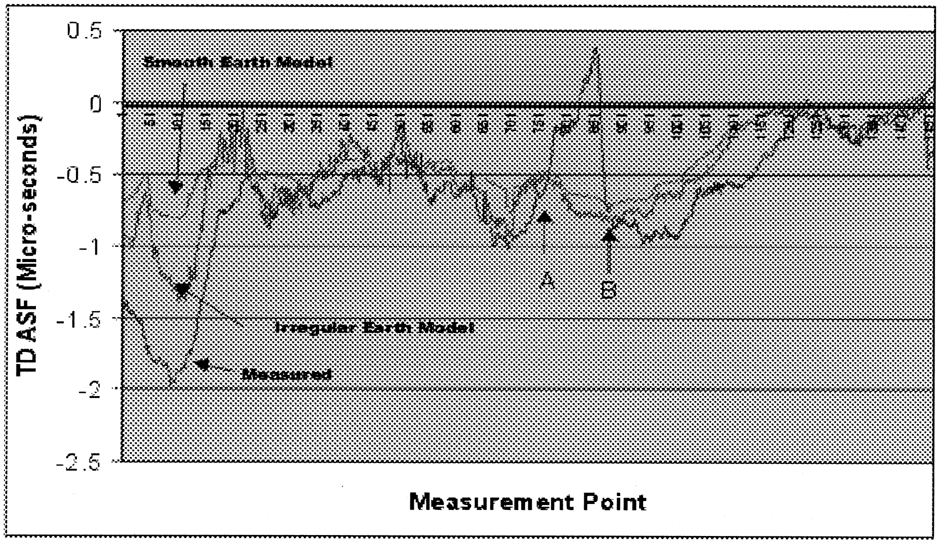

Figure 8. Comparison of measured TD ASF data with smooth earth model and irregular earth model results.

(smaller intervals). We carefully investigated the effects of varying the integration interval, using the exceptionally-demanding land path in the above example. For convenience of calculation, all intervals tested were multiples of the 90 m terrain elevation database resolution. Increasing the interval from 90 m, the errors rapidly climbed from a few nanoseconds to unacceptable values as the interval exceeded 630 m, so this value was chosen for future use. The change results in approximately a 50 times increase in the speed of computation!

6. COMPARISON OF MODELLED ASFs WITH MEASURED DATA. At the time of writing, no TOA ASF measurements have been collected from our proposed *difficult* trials area that lies around the Test Point shown in Figure 3(a). However, in 1996 and 1997 the General Lighthouse Authorities (GLAs) of the United Kingdom and Ireland carried out sea-trials aboard the vessel *MV Pharos*, to investigate the coverage of UK waters by NELS. The trial routes included one off the west coast of Scotland, served by Loran-C signals from Vaerlandet, Sylt and Ejde that had propagated across mountainous terrain. The equipment on the vessel included two Loran-C receivers and a DGPS receiver. Although the set-up was not suitable for making the precise ASF measurements we will require, and the results are TD, not TOA, ASFs, the records do allow us to compare the ASFs generated by our new *difficult* area model with measured data.

The section of route shown in Figure 7 is approximately 100 km long. It runs through the Sound of Mull, a seaway some 2 km wide between mountains that rise to between 500 and 750 m above sea-level. We have extracted ASF values by calculating the differences between the TD values recorded on the ship using Ejde (Faroes) and Vaerlandet (Norway), and the corresponding TD values we calculated from the ship's DGPS positions using the Salt-Water model. Figure 8 compares these measured ASF values with those generated by our new *irregular Earth* model. Results generated by our earlier *smooth Earth* model are also included. The test equipment,

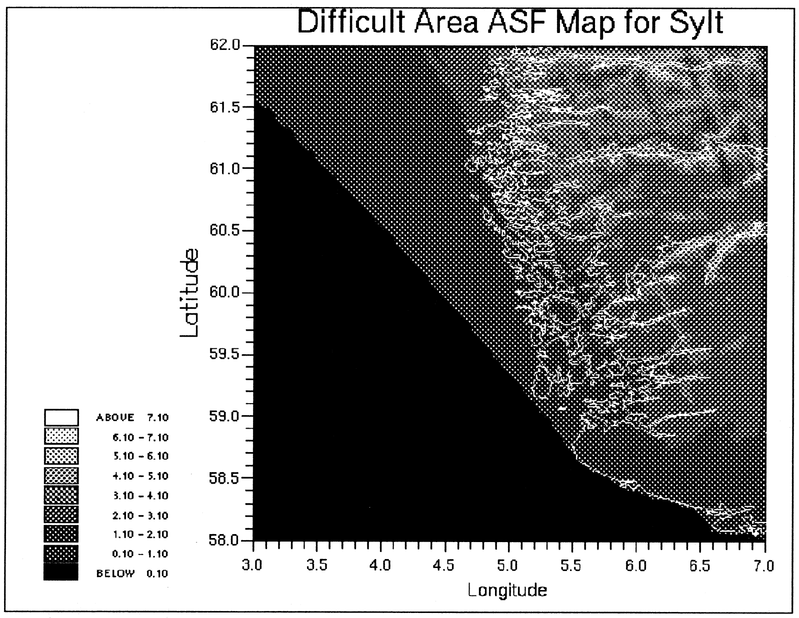

Figure 9. ASFs of the *difficult* Norwegian coast generated by the irregular earth model.

however, was not designed with precise synchronisation between DGPS and Loran data. It was thus subject to velocity errors. These do not invalidate the use of the data to compare the shapes of ASF profiles provided the ship steams with reasonably consistent speed and heading, as it did through the Sound of Mull and out to sea. But when it temporarily changed heading on leaving the Sound, A–B in Figure 8, an error resulted.[5] We have omitted this short part of the record from our analysis of the data.

The irregular Earth model results fit the measured data with an rms error of 282 ns. As would be expected in an area of rapid topographical variation, these results are better than those from the simpler smooth Earth model, for which the rms error is 386 ns. But of greater importance is the degree of agreement between the shapes of the curves, since wide-area discrepancies are removed in our ASF-mapping method by the process of adjusting the modelled results to fit the measurements at widely-spaced points. We simulated this process by removing the mean difference between the measured and irregular Earth data sets, 193 ns. Doing this should also have removed any shift due to constant-velocity effects.

The result was a fall in the rms discrepancy between the two data sets to 234 ns. This is an estimate of the accuracy with which the *irregular Earth* model can predict the variations of the TD ASFs in this region. It is an encouraging result and we await a higher-quality set of TOA ASF data with anticipation. It will allow us to specify the nature and degree of the surveying and calibration methodology to be employed in mapping ASFs in *difficult* areas.

7. MAPPING *DIFFICULT* AREA MODELLED ASFS. Figure 9 shows a two-dimensional map, in the form of a contour plot, of the TOA ASFs of the signals from Sylt, generated using the new *irregular Earth* model. It covers the whole of the *difficult* sea-trial area and beyond. Sylt lies several hundred kilometres south of the

south-east corner of the area shown (Figure 3). The ASF values are, of course, zero off the coast where the signal has travelled via an all-sea path. As one comes ashore it increases rapidly, with the increasing component of land in the path. The greatest ASF values in this area outside the steep-sided, deep, fjords are of the order of 3–4 μs; in the fjords we have seen that they may reach 6–7 μs. The corresponding position errors if no compensation is applied to such ASFs are in the range 1–2·5 km.

8. FURTHER WORK. The development of the *irregular Earth* model described in this paper completes the process of developing computer ASF models. In the near future, hardware should be available that will allow trials to be conducted in the *difficult* test area. The results will be compared in detail with the predictions of the *smooth Earth* and *irregular Earth models*. This will establish how close together the sparse data points used for adjustment of the results need to be. Software to carry out the process of calibrating ASFs, by adjusting the fine-detailed results produced by the modelling process to best-fit sparse data, has been developed and tested. Thus a working software suite now exists for all parts of the operation.

However, an alternative, and potentially improved, method of calibrating *difficult* area ASFs by using a Kalman filter is currently under investigation. Rather than using the measured data to adjust the modelled data directly, in the Kalman filter method we adjust the coefficients of a two-dimensional polynomial that represents the differences between the modelled and the measured values. This Kalman approach lets us cater for the variations in the noise components of the measured ASF values such as those expected when the survey vessel sails into fjords in mountainous terrain where substantial signal attenuation is likely to be experienced.

When the final ASF data set for the whole of NELS has been produced, it will be published for use by equipment manufacturers and others in formats compatible with the memory requirements of Loran-C receivers, or those of integrated navigation systems. With conventional methods of storage, it is straightforward to convert between the various formats preferred by Loran-C receiver manufacturers. However, the amount of data is considerable, and we are investigating the use of neural networks as a high-density storage technique. One type of neural network being studied would allow the stored ASFs to be adjusted online to account automatically for the small variations that occur between seasons of the year.

9. SUMMARY AND CONCLUSIONS. This paper has reviewed the *Mapping ASFs for NELS* project at Bangor. It has presented an important recent advance, the development of a model for predicting ASFs in areas of irregular terrain. The new model is based on Monteath's method of solution of an integral-equation technique for modelling phase delays in mountainous regions. In the paper, we illustrate the use of the technique by citing the example of a path in a mountainous region of Norway, showing the terrain profile and the resulting ASF variations. The profound effects of the topography on Loran-C propagation across a deep fjord (probably the most difficult region within the NELS coverage area) are clearly illustrated. The results of the model are also compared with data recorded in a mountainous coastal area of western Scotland. The results of this comparison indicate good agreement between the measured and modelled results even before calibration.

REFERENCES

[1] *Specification of the Transmitted Loran-C Signal*. (1994). United States Coast Guard, Department of Transportation, COMDTINST M16562.4

[2] Johler, J. R, Kellar, W. J. and Walters, L. C. (1956). *Phase of the Low Radio Frequency Ground Wave*. NBS Circular 573, NBS, June.

[3] Melgård, T. E. and Last, J. D. *ASF Mapping of NELS Preliminary Phase*. Report of contract number: NODECA/93/5107/30, School of Electronic Engineering and Computer Systems, University of Wales, Bangor, Gwynedd, UK.

[4] Williams, P. and Last, J. D. (1998). *NELS ASF Demonstration Phase: Report at 10 January 1998*. School of Electronic Engineering and Computer Systems, University of Wales, Bangor, UK.

[5] Williams, P and Last, J. D. (1998). Mapping Additional Secondary Factors for the North-West European Loran-C chains—initial results and further work. *27th Annual Convention and Technical Symposium*, *International Loran Association*, Danvers, Mass. USA, 11–15 Oct.

[6] Millington, G. (1949). Ground-wave propagation over an in-homogeneous smooth Earth. *Proceedings of the IEE*, Series 96, Number 3, p. 53.

[7] Pressey, B. G., Ashwell, G. E, and Fowler, C. S. (1952). The measurement of the phase velocity of ground-wave propagation at low frequencies over a land path. *Proceedings of the IEE*, Series 100, Number HI, pp. 73–84.

[8] *World Atlas of Ground Conductivities* (1988). CCIR Report 717-2, Geneva.

[9] *Defense Mapping Agency Product Specifications for World Vector Shoreline* (1988). DMA Hydrographic/Topographic Center, Washington, DC.

[10] Williams, P and Last, J. D. (1997). Mapping additional secondary factors for the North-West European Loran-C chains. *26th Annual Convention and Technical Symposium*, *International Loran Association*, Ottawa, Canada, 6–9 Oct.

[11] Wait, J. R. (1964). Electromagnetic surface waves. In *Advances in Radio Research* (ed. Saxton, J. A.), Academic Press, London.

[12] Wait, J. R. (1962). Propagation of electromagnetic waves along the Earth's surface. In *Electromagnetic Waves* (ed. Langer, R. E.), University Press, Wisconsin.

[13] Maclean, T. S. M and Wu, Z. (1993). *Radiowave Propagation Over Ground*. Chapman & Hall, London.

[14] Monteath, G. D. (1978). Computation of groundwave attenuation over irregular and inhomogeneous ground at low and medium frequencies. *BBC Report 1978/7*, British Broadcasting Corporation, Research and Development, Kingswood Warren, Tadworth, Surrey, UK.

[15] Hufford, G. A. An integral equation approach to the problem of wave propagation over an irregular terrain. *Q. J. Appl. Math.* **9**(4), 391–404.

[16] Johler. J. R. *et al*., (1967). Loran-D phase corrections over inhomogeneous irregular terrain. *Report ITSA 56*, Institute for Telecommunication Sciences and Aeronomy, Boulder, Colorado, November 1967.

[17] Samaddar, S. N. (1979). The theory of Loran-C ground wave propagation – a review. *Navigation*, the Journal of The US Institute of Navigation, **26**, (3) 173–187.

[18] Performance specification Digital Terrain Elevation Data (DTED) (1996). Project MCGT-0194, *Document MIL-PRF-89020A*, National Imagery and Mapping Agency, Bethesda, Maryland, USA.

https://doi.org/10.1017/S0373463300008778 Published online by Cambridge University Press